Chapter 12
Shoreline Extrapolations

Jean Serra

Abstract A morphological approach for studying coast lines time variations is proposed. It is based on interpolations and forecasts by means of weighted median sets, which allow to average the shorelines at different times. After a first translation invariant method, two variants are proposed. The first one enhances the space contrasts by multiplying the quench function, the other introduces homotopic constraints for preserving the topology of the shore (gulfs, islands).

Keywords Median sets · Binary interpolation · Hausdorff distances · Shoreline Time forecasting

12.1 Three Problems, One Theoretical Tool

The following study holds on lagoon inlets movements. It extends and develops an experimental study made by N.V. Thao and X. Chen about Thuan An Inlet Area (Thao and Chen 2005). The predictions proposed by these authors were obtained by averaging over the time the successive positions of a complex shoreline, including lagoon inlets, which results in a prediction of the coast line. J. Chaussard showed, in Chaussard (2006), that this prediction correctly fits with ulterior data from Google Earth (see Fig. 12.1).

In Thao and Chen (2005), the authors used a popular way to estimate accretions (Srivastava et al. 2005). Figure 12.2 depicts this semi-manual approach: the shoreline has been discretized into segments which are shifted upwards according a given accretion law (here the linear law $y = ax + b$, where x stands for the time). Indeed, this is nothing but a sampled version of the dilation the shoreline by the disc of radius $ax + b$. Such a circular dilation of a shoreline turns out to be the simplest expression of its evolution under an accretion process, since it is uniform everywhere and does not take the previous stages of the shoreline into account. As a matter of fact, the

J. Serra (✉)
Ecole des Mines de Paris, Paris, France
e-mail: jean.serra@cmm.ensmp.fr

B. S. Daya Sagar et al. (eds.), *Handbook of Mathematical Geosciences*,
https://doi.org/10.1007/978-3-319-78999-6_12

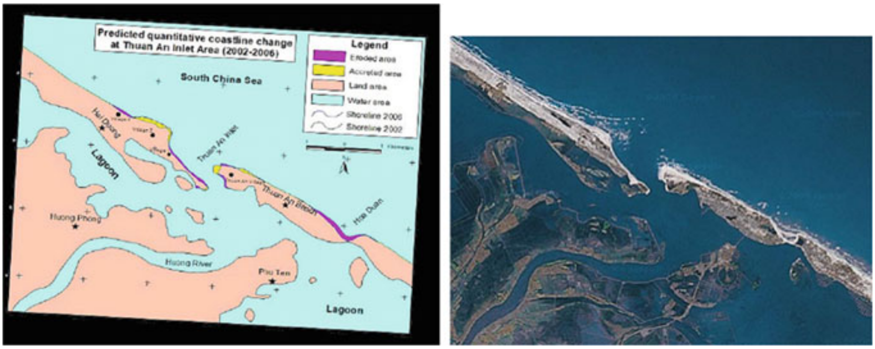

Fig. 12.1 Left: Lagoon Inlets forecast by N.V. Thao and X. Chen; right: Current Google earth view of the same area

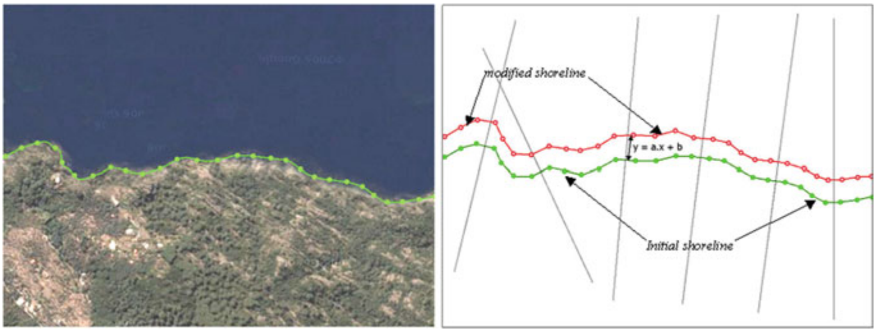

Fig. 12.2 Classical semi-manual technique of extrapolation

notion of a set extrapolation is not straightforward, and depends considerably on the features one wishes to preserve or to emphasize.

1. If, by comparing the shorelines at years n and $n-1$, there appear zones of erosion[1] and zones of accretion, we may require a forecast of the shoreline, at year $n+1$, to pursue erosions and accretions, but always in the same zones as previously; moreover, we must be able to express several laws for this time evolution (for example, in Thao and Chen 2005, a linear and a logarithmic laws are discussed);
2. if we know the movements of the shore during the last ten years, with one map per year, we can average these ten sets independently of their dates and base the extrapolation on this average only, or we can alternatively emphasize the more recent maps, considering that the last one, or the last two ones, carry most of the information;

[1]The shoreline context, the two words of "erosion" and "accretion" refer to the two types of changes depicted in Fig. 12.3. The word "erosion" also appears in the context of mathematical morphology, for naming the operation $\ominus$ involved in Eq. 12.1. It is pure coincidence.

3. if the shore exhibits small gulfs, islands and lagoon lakes, we may require from the extrapolation to preserve their homotopy, i.e. neither to create new islands (new gulfs, new lakes) nor to suppress the existing ones.

The first two questions can be treated within the framework of the median set theory, and the third one reduces to a small variant. Though median elements were thoroughly studied for interpolation problems, by M. Iwanowski in particular Iwanowski and Serra (2000) no attention was paid to their potentialities for generating averages and extrapolations. We believe nevertheless median sets turn out to be convenient tools for shorelines forecast, which in addition extend directly to numerical functions (however, we shall not treat the numerical extension here, and restrict ourself to the binary approach).

What follows is an attempt in this direction. After a presentation of the median set, that we adapt to shorelines in Sect. 12.2, we analyze in Sect. 12.3 a series of derived notions, such as weighted median set, quench function and quench stripe, and averages. The heart of the matter is treated in Sect. 12.4, where various laws are proposed for the dynamics of the coast movements. A short section on homotopy preservation precedes the conclusion. All images of coasts which are used below are *simulations*, and have the same digital size of 512×320 pixels.

12.2 Median Set

In literature, median set appears as an interpolation algorithm in Casas (1996) and in Meyer (1996), and was extended to partitions in Beucher (1998). Its formal definition and its basic properties were given in Serra (1998). Since, the approach has been developed by several authors (Angulo and Meyer 2009; Charpiat et al. 2006). In what follows, the geographical space is modelled by the Euclidean plane, but the approach applies as well to any metric space, including the digital ones. The model of Euclidean median sets does not concern the *lines* of the shores, but the *whole landsets*, whose the shorelines are the boundaries. These landsets, denoted below by A_1, A_2, etc., are depicted for example in Fig. 12.3 left, whereas the only shorelines boundaries, in another example, are depicted in Fig. 12.5 left. The basic results we need to start with are the Definition 1 of a median set, and the two properties 2 and 3, drawn from Serra (1998).

Hausdorff distance ρ concerns the class $\mathscr{K}'$ of the noncompact sets of R^n (here of R^2). It is the mapping $\rho : \mathscr{K}' \times \mathscr{K}' \to R_+$

$$\rho(X, Y) = \inf\{\lambda : X \subseteq Y \oplus \lambda B ; Y \subseteq X \oplus \lambda B\} \qquad (12.1)$$

where B designates the unit disc centered at the origin, and where $\oplus$ and $\ominus$ designate Minkowski addition (or dilation) and substraction (or erosion) respectively.

Consider now an *ordered* pair of closed sets $\{X, Y\}$, with $X \subseteq Y$, and such that the numerical value $\rho(X, Y)$, as given by Eq. (12.1), is finite. Their median element is defined as follows:

Definition 1 The median element between the two ordered sets $X, Y \in \mathcal{K}'$, with $X \subseteq Y$, is the compact set $M(X, Y)$, comprised between X and Y and whose boundary points are equidistant from X and Y^c.

In other words, the boundary ∂M of M is nothing but the skeleton by zone of influence, or *skiz*, between X and Y^c.

Proposition 1 *The median set between X and Y is obtained by taking the union*

$$M(X, Y) = \cup\{(X \oplus \lambda B) \cap (Y \ominus \lambda B)\ \lambda \geq 0\} \tag{12.2}$$

where the λ can be limited to the values smaller or equal to

$$\mu = \inf\{\lambda : \lambda \geq 0,\ X \oplus \lambda B \supseteq Y \ominus \lambda B\} \tag{12.3}$$

and where the equality is reached for at least one point of ∂M.

Proof A point m at a distance $\leq \lambda$ from X and $\geq \lambda$ from Y^c belongs to set $(X \oplus \lambda B) \cap (Y \ominus \lambda B)$, hence to set of Eq. (12.1). Conversely, as every point $m \in M$ belongs to at least one term of the union, there exists a $\lambda \geq 0$ with $d(m, X) \leq \lambda$ and $d(m, Y^c) \geq \lambda$, which results in Eq. (12.1). As for Eq. (12.2), we observe that for λ large enough we have $(X \oplus \lambda B) \cup (Y^c \oplus \lambda B) = R^2$ because set Y is bounded. These λ bring no contribution to set $M(X, Y)$, since $X \oplus \lambda B \supseteq Y \ominus \lambda B$. Finally, for $\lambda = \mu$, we obtain a point of the boundary ∂M because X and Y are closed, which achieves the proof.

Here is now an instructive property which shows how both Hausdorff distances by dilation and by erosion[2] are involved in the median $M(X, Y)$ (Serra 1998).

Proposition 2 *Given $X, Y \in \mathcal{K}'(R^n)$, the median element $M(X, Y)$ is at Hausdorff dilation distance μ from X and from the closing $X \bullet \mu B = (X \oplus \mu B) \ominus \mu B$, and at Hausdorff erosion distance μ from Y and from the opening $Y \circ \mu B = (Y \ominus \mu B) \oplus \mu B$.*

[2]Hausdorff distance σ for erosion, introduced in by the relation

$$\sigma(X, Y) = \inf\{\lambda : X \ominus B_\lambda \subseteq Y\ ;\ Y \ominus B_\lambda \subseteq X\}$$

concerns the subclass $\mathcal{A}$ of $\mathcal{K}'(E)$ of the regular compact sets, i.e. such that $\overline{X^o} = X$. It is indeed a distance on $\mathcal{A} \times \mathcal{A}$. If $\sigma(X, Y) = 0$, then we have

$$Y \supseteq \bigcup_{\lambda>0} X \ominus B_\lambda = X^o \Rightarrow Y \supseteq \overline{X^o} = X \qquad X, Y \in \mathcal{A}$$

and similarly $X \supseteq Y$, hence$X = Y$ (the other two axioms are proved as for distance ρ) (Serra 1998).

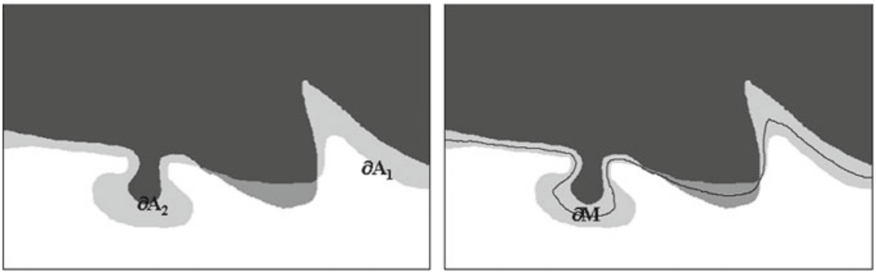

Fig. 12.3 Left: two simulated shore images A_1 and A_2. The older is supposed to be A_1 (the white one).The zones of accretion from A_1 to A_2 are in light grey, those of erosion in dark grey; right: the boundary of the median set M between A_1 and A_2

The Hausdorff distance applies to non empty compact sets. But clearly, the landsets under study are not empty, and the above assumption that $\rho(X, Y) < \infty$ comes back to say that all involved distances are bounded.

12.3 Median and Average for Non Ordered Sets

Non ordered sets In general, two successive shores A_1 and A_2 are not ordered, i.e. their change comprises both erosions and accretion areas. If so, the previous results do not apply to two A_1 and A_2 directly, but to their intersection $X = A_1 \cap A_2$ and their union $Y = A_1 \cup A_2$ which are ordered since $X \subseteq Y$. Equation (12.1) of the median element becomes

$$M(A_1, A_2) = \bigcup_{\lambda \geq 0} [A_1 \cap A_2) \oplus \lambda B] \cap [(A_1 \cup A_2) \ominus \lambda B] \tag{12.4}$$

Figures 12.3 depicts an example of median set M. One observes that ∂M goes through all points where the two coastlines intersect. The property is general, since these points belong to both $A_1 \cap A_2$ and $A_1 \cup A_2$.

Weighted median Set M is said to be *median* because each point of ∂M is equidistant from X and Y^c, which is a consequence of the same weight given to dilation and erosion in Eq. (12.2). By changing this weight, i.e. by replacing M by

$$M_\alpha(X, Y) = \bigcup_{\lambda} \{(X \oplus \alpha\lambda B) \cap (Y \ominus (1 - \alpha)\lambda B)\} \tag{12.5}$$

for a $\alpha \in [0, 1]$, we generate another interpolation, and by making α vary, a series of progressive interpolations from X to Y (Huttenlocher 1995), all the closer to set Y since α is high. One will notice that when the two shores A_1 and A_2 are *not* nested in each other, then one takes for the two operands of Eq. (12.5) $X = A_1 \cap A_2$ and

$Y = A_1 \cup A_2$. This provides interpolators such as those of Fig. 12.4. Unfortunately, these interpolators are closer to the highest or to the lowest line, no matter these lines are portions of ∂A_1 or of ∂A_2. For correcting this drawback, one must take the interpolator M_α in the zones where A_1 is larger than A_2 (for example), and $M_{1-\alpha}$ in the other ones. Denoting by $N(A_1,\ A_2)$ the correct weighted interpolator, we now have

$$N_\alpha(A_1,\ A_2) = M_{1-\alpha}(A_1,\ A_2)\ when\ A_1 \backslash A_2 \neq \emptyset \qquad (12.6)$$
$$= M_\alpha(A_1,\ A_2) when\, A_2 \backslash A_1 \neq \emptyset$$

Figure 12.5 depicts such corrected interpolators.

The physical equation of the phenomenon Physically speaking, the accretion/erosion process evolves at each instant from the stage it has reached before. It takes some $M_\alpha(X,\ Y)$, with $\alpha \in [0, 1]$, as starting point and moves to $M_\beta[M_\alpha(X,\ Y),\ Y]$, for some value $\beta \in [0, 1]$. The weighted medians M_α do model this evolution because they form a semi-group. By calculating firstly the set $M_\alpha(X,\ Y)$ median between X and Y, and then the set $M_\beta[M_\alpha(X,\ Y),\ Y]$ between $M_\alpha(X,\ Y)$ and Y, we obtain indeed the same result as by calculating directly $M_\gamma(X,\ Y)$ for the weight $\gamma = \alpha + (1 - \alpha)\beta = \alpha + \beta - \alpha\beta$, i.e.

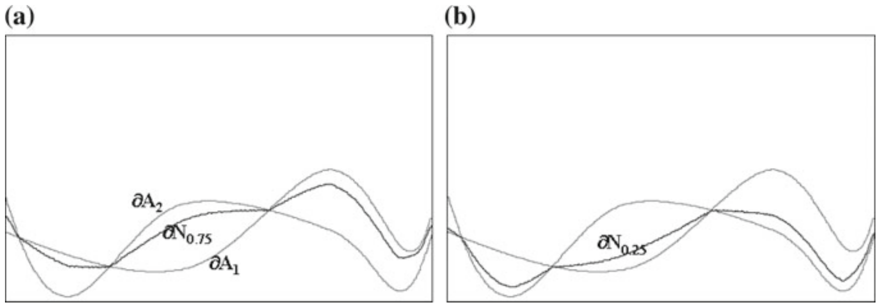

Fig. 12.4 Raw weighted median lines

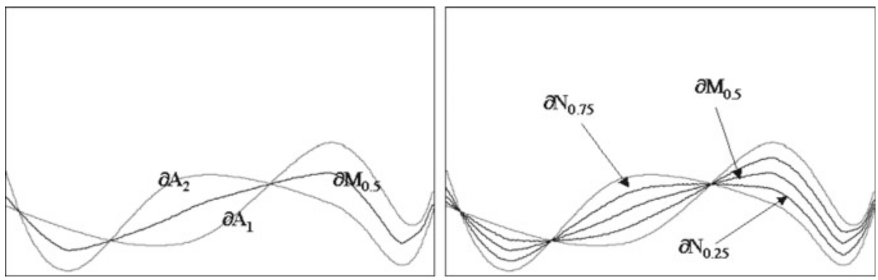

Fig. 12.5 Left: two shores A_1 and A_2, of boundaries ∂A_1 and ∂A_2, and their median line of boundary $\partial M_{0.5}$; right: the same, plus two additional weighted median lines according to Eq. (12.5)

$$M_\beta[M_\alpha(X,\ Y),\ Y] = M_{\alpha+\beta-\alpha\beta}(X,\ Y) \tag{12.7}$$

For example, in Fig. 12.5 right, the three median sets correspond to $\alpha = 0.75, 0.5$, and 0.25, and the weighted median $M_{0.75}$ is *also* the median element between $M_{0.5}$ and $A_1 \cup A_2$.

Proposition 3 *Given* $X,\ Y \in \mathscr{K}'(R^n)$, *the family* $\{M_\alpha(X,\ Y), 0 \le \alpha \le 1\}$ *of median elements form an additive semi-group for the addition* $\alpha \otimes \beta = \alpha + \beta - \alpha\beta$.

Proof Clearly, $\alpha \otimes \beta \in [0, 1]$, *thus Eq.* (12.7) *defines a commutative semi-group. The operation* $\alpha \otimes \beta$ *is also associative, since*

$$\gamma \otimes (\alpha + \beta - \alpha\beta) = \gamma + \alpha + \beta - \alpha\beta - \gamma\alpha - \gamma\beta + \gamma\alpha\beta$$

is symmetrical in α, β, γ, *therefore* $\alpha \otimes \beta$ *is an algebraic addition.*

Quench function and quench stripe As a matter of fact, the median operator provides *two outputs*, since we have on the one hand the (weighted or not) *median set M*, whose contour ∂M is the dark middle line in Fig. 12.5 left, or Fig. 12.6 left, and the *quench function q*, defined on ∂M and which gives at each the radius of the minimum disc hitting the two contours ∂A_1 and ∂A_2.

$$q(z) = \inf\{r : B_z(r) \cap \partial A_1 \neq \emptyset \text{ and } B_z(r) \cap \partial A_2 \neq \emptyset\} \tag{12.8}$$

A few of such discs, for the two inputs A_1 and A_2 of Fig. 12.3 left, are depicted in Fig. 12.6 left, and their union for the whole quench function gives the *quench stripe w*, i.e. the dark grey stripe W around the black line ∂M in Fig. 12.6 right, with

$$W = \cup\{B_z(q(z)),\ z \in M(A_1,\ A_2)\} \tag{12.9}$$

Note hat this dark grey stripe does not reach the edges of input sets A_1 and A_2, but an open version of their union, and a closed version of their intersection.

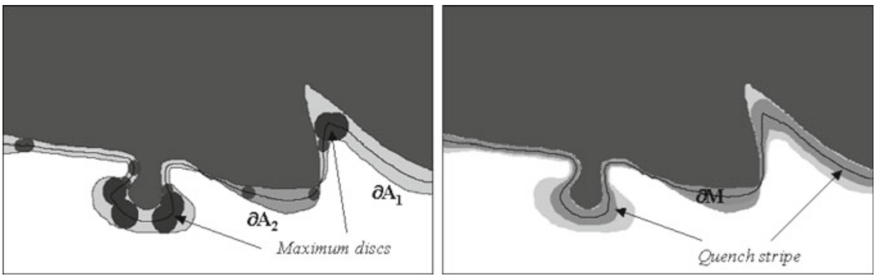

Fig. 12.6 Left: a few maximum discs centered on the median line; right: the dark grey stripe is the union of all maximum discs, or "quench stripe"

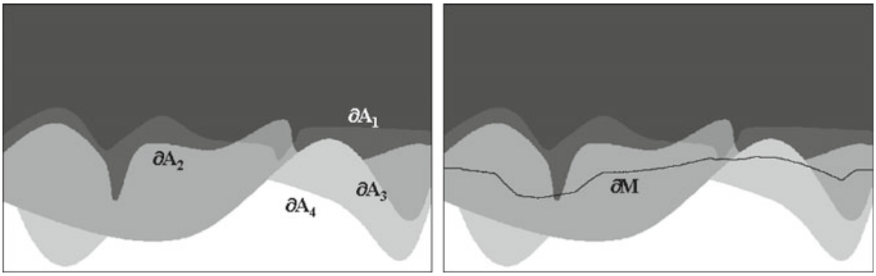

Fig. 12.7 Left: four shores; right in dark, their median line

Averages The structure of Eq. (12.7) suggests a technique for extending the median element to more than two input sets. Starting for example from the triplet $\{A_1, A_2, A_3\}$, we can calculate $M_{0.5}(A_1, A_2)$ in a first stage, and then $M_{0.33}[M_{0.5}(A_1, A_2), A_3]$. The resulting median element averages the three inputs, in a median sense. Figure 12.7 depicts an example of such an average for the four inputs $\{A_1, ..A_4\}$ shown in Fig. 12.7 left (two of them are the sets involved in Fig. 12.5 left). The initial stage consists in calculating $M_{0.5}(A_1, A_2)$ and $M_{0.5}(A_3, A_4)$, and the final one in calculating $M_{0.5}[M_{0.5}(A_1, A_2), M_{0.5}(A_3, A_4)]$, a set whose contour is drawn in black in Fig. 12.7 right. This final result is independent of the choice of the sets in the initial stage, and we could start as well from $M_{0.5}(A_1, A_3)$ and $M_{0.5}(A_2, A_4)$.

The averages obtained this way blur the structural features of the shores. Imagine for example that A_2, A_n are shifted versions of A_1 in the horizontal direction. As n increases, the median average contour tends towards an horizontal line: all features, gulfs, capes, etc. are lost. We meet here the same trouble as in interpolating moving objects, with translation and rotation. In case of shore movements, the translations are probably less intense, but the problem still remains. Remark also that this drawback is the counterpart of the advantage of preserving accretion and erosion zones.

12.4 Extrapolations via the Quench Function

In this section and the next one, we focus on the extrapolation of two shores at most, A_1 and A_2 say. If we dispose of a chronological sequence of the coast movements, A_1 and A_2 stand for the last two observations, A_2 being the more recent. The principle of the extrapolation consists in two possible changes:

1. that of the quench function according to a given law, which models the dynamics of the movement, and which results in a new quench stripe W;
2. that of the respective importances of A_1 and A_2. If we take the median $M_{0.5}(A_1, A_2)$, then both shores are given the same weight, but if we consider that A_2, more recent, is two times more significant than A_1, then we can take $N_{0.66}(A_1, A_2)$.

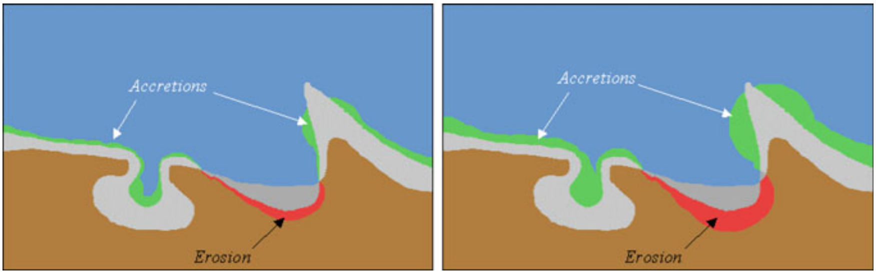

Fig. 12.8 Two extrapolations of the shoreline of Fig. 12.3; both are centered on $\partial M_{0.5}(A_1,\ A_2)$; the quench function is multiplied by 2 in the left image and by 3 in the right one

Fig. 12.8 depicts two extrapolations where the median element equals $M_{0.5}(A_1,\ A_2)$, hence where the two input shores are given the same importance, but where the quench stripe W of Eq. (12.9) is replaced by

$$W = \cup\{B_z(kq(z)),\ z \in M_{0.5}(A_1,\ A_2)\}$$

The radius of the disc centered at each point of $M_{0.5}(A_1,\ A_2)$ is quench value multiplied by factor k, with $k = 2$ for Fig. 12.8 left and $k = 3$ for Fig. 12.8 right. We see that, as k increases, both accretion and erosion zones are developed. We can also notice that the shape of the cape provokes a bizarre inflation in Fig. 12.8 right.

This swelling may be due to the great distance from the median line to extremity of the cape, as shown in Fig. 12.6 right, so that we can try to avoid it by making the median line closer to contour ∂A_2 which delineates the cape. Replace then the median set $M_{0.5}(A_1,\ A_2)$ by $N_\alpha(A_1,\ A_2)$, in the sense of Eq. (12.6), with $\alpha = 0.75$, so that the quench stripe becomes

$$W = \cup\{B_z(kq(z)),\ z \in N_{0.75}(A_1,\ A_2)\}.$$

The resulting changes are depicted in Fig. 12.9, left for $k = 3$, and right for $k = 4$. By comparing Figs. 12.8 right and 12.9 left where the quench function is multiplied by the same value $k = 3$, we see that the cape inflates less, but in compensation the erosion zone vanished. The erosion can reappear by taking $k = 4$ (Fig. 12.9 right), but again the cape inflates as strongly as in the previous extrapolation of Fig. 12.8 right.

In fact, transforming a quench function according to pure magnification is probably too poor. One can easily imagine more sophisticated laws such as the two following ones:

1. the median line is slightly moved toward the second contour, by taking $N_{0.66}(A_1,\ A_2)$, and the quench stripe W is obtained by dilating each point z of the median line by the disc of radius $2q(z)$ and by the segment $L_\alpha(2q(z))$ of length $2q(z)$ in the main direction α of the cape, which gives

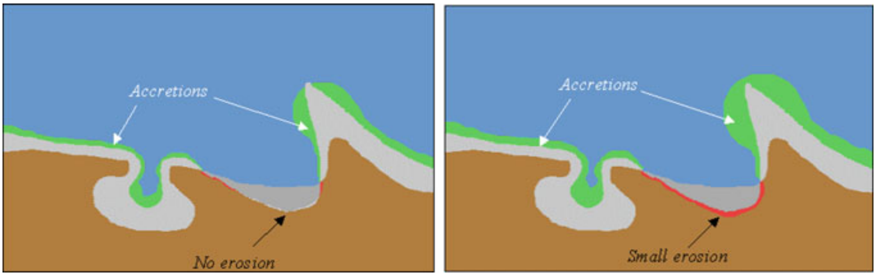

Fig. 12.9 Two other extrapolations of the shoreline of Fig. 12.3; both are centered on $\partial N_{0.75}(A_1, A_2)$; the quench function is multiplied by 3 in the left image and by 4 in the right one

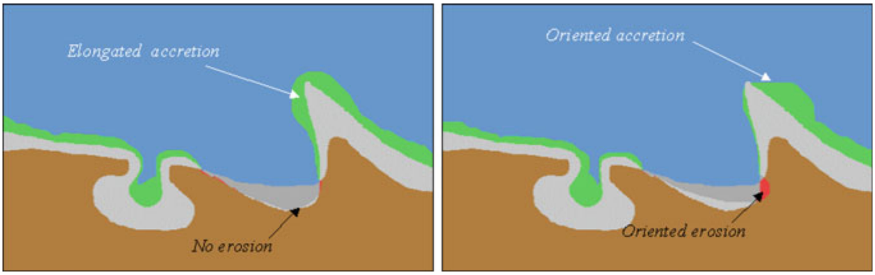

Fig. 12.10 Two extrapolations of the shoreline of Fig. 12.3, by emphazising the new capes in the left image, and by introducing an east-west trend in the right one

$$W = \cup\{[B_z(2q(z) \oplus L_\alpha(2q(z))],\ z \in N_{0.66}(A_1, A_2)\}$$

and which is depicted in Fig. 12.10 left. The accretion around the cape turns out to be now more realistic, but the erosion zone has disappeared.

2. The median set $N_{0.66}(A_1, A_2)$ is left unchanged, and a supplementary trend in the horizontal direction is introduced by a dilating points z by the horizontal segment $L_0(3q(z))$. For avoiding too fast changes, the parameters of the two other dilations are divided by 2. The shifting effect of the trend operation appears clearly in Fig. 12.10 right, where the accretion forms a deposit at the east of the cape. Similarly, the directional effect of the erosion holds for west oriented regions.

Unlike the previous models, which all are invariant under rotation of the map, these last two laws, which model marine currents, depend on the North direction (see Fig. 12.10).

12.5 Accretion and Homotopy

It may happen that, for some reasons, one wishes to preserve the homotopy of the shore, which excludes the creation, or the suppression, of lakes and islands. Now, by dilating enough the shore of Fig. 12.10, we risk to close the gulf on the left and to generate in internal island. An easy way to protect the gulf as such consists in replacing the dilation w.r.t. the unit disc by a cycle of elementary homotopic thickenings in the eight directions of the square grid, or the six ones in the hexagonal case (Serra 1982). The circular dilation of size n becomes the series of n thickening cycles. One can see in Figure ll, left and right, the results of two thickenings of sizes 25 and 33 respectively (for a 512×320 digital image). The gulf is preserved by a narrow channel, which could be enlarged by modifying the homotopy preservation algorithm. This conceptually simple method is not the only possible one. In Vidal et al. (2005) the authors propose a median set based interpolation that preserves particles by marking them by a homotopic thinning, and translating them during the interpolation process.

12.6 Conclusion

Our purpose was to demonstrate the physical sense of the median set approach and its flexibility. In the first section, we indicated three features to be respected by interpolations. According to the first one, an accretion (resp. erosion) zone must continue to evolve by accretion (resp. erosion). This basic modality is fulfilled by all models of Sect. 12.4. The laws proposed in this section are far from being the only possible ones. In particular, each of the six examples of the section is given a same law for accretion and erosion, which is not at all an obligation. The second feature holds for the role of the past. In the approach of Sect. 12.4, this past reduces to the last two stages: they suffice to determine the starting shoreline, the “gradient”, and the location of accretion/erosion (Fig. 12.11).

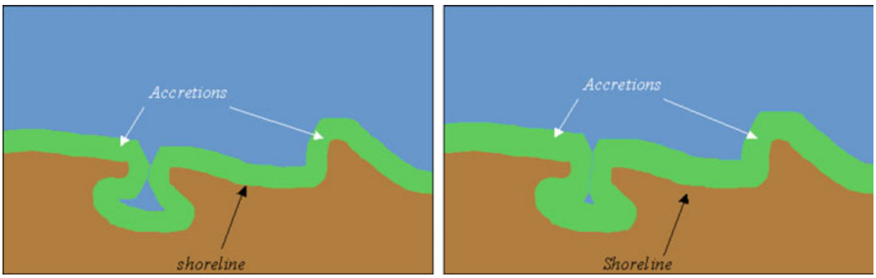

Fig. 12.11 Two extrapolations of the shoreline of Fig. 12.3 by homotopic thickenings of sizes 25 (left) and 33 (right)

The third feature was the subject of Sect. 12.5, where a thickening is substituted for the dilation in the extrapolator, in order to preserve homotopy. Indeed, all extrapolation equations, from sections two to four, can be rewritten by replacing the unit disc erosion and dilation by unit cycles of thinnings and thickenings, and the linear dilations by unidirectional thickenings. It would result in a series of algorithms where increasingness is lost (non direct extension to numerical functions) but where topological features are preserved.

Finally, as the weighted median of Eq. (12.4) is an increasing function of its two operands, it extends to numerical functions by means of their subgraphs, and allows to process colour images (Daya Sagar 2007).

Acknowledgements I am extremely grateful to Dr B.R. Kiran for his precious help in preparing this chapter.

References

Angulo J, Meyer F (2009) Morphological exploration of shape spaces. In: Wilkinson MHF, Roerdink JBTM (eds) Mathematical morphology and its applications to signal and image processing. Springer, Berlin, pp 226–237

Beucher S (1998) Interpolation of sets, of partitions and of functions. In: Heijmans H, Roerdink J (eds) Mathematical morphology and its applications to image and signal processing. Kluwer, Dordrecht

Casas JR (1996) Image compression based on perceptual coding techniques, PhD thesis, UPC Barcelona, March 1996

Charpiat G, Faugeras O, Keriven R, Maurel P (2006) Distance-based shape statistics. IEEE ICASP 5:925–928

Chaussard J (2006) Surveillance cotire l'aide de la morphologie, a bibliographical study, A2SI, ESIEE France

Daya Sagar BS (2007) Universal scaling laws in surface water bodies and their zones of influence. Water Resour Res 43(2):W02416

Huttenlocher DP, Klunderman GA, Rucklidge WJ (1995) Comparing images using the Hausdorff distance. IEEE PAMI. 15(9)

Iwanowski M, Serra J (2000) The morphological-affine object deformation. In: Goutsias J, Vincent L, Bloomberg DS (eds) Mathematical morphology and its applications to image and signal processing. Kluwer Academic Publisher, Dordrecht, pp 81–90

Meyer F (1996) A morphological interpolation method for mosaic images. In: Maragos P et al. (eds) Mathematical morphology and its applications to image and signal processing. Kluwer, Dordrecht

Serra J (1982) Image analysis and mathematical morphology. Academic Press, London

Serra J (1998) Hausdorff distance and Interpolations. In: Heijmans H, Roerdink J (eds) Mathematical morphology and its applications to image and signal processing. Kluwer, Dordrecht

Srivastava A, Niu X, Di K, Li R (2005) Shoreline modeling and erosion prediction. In: proceedings of the ASPRS annual conference

Thao NV, Chen X (2005) Temporal GIS for monitoring lagoon inlets movements. In: Chen X (ed) DMAI' 2005. AIT Bangkok

Vidal J, Crespo J, Maojo V (2005) Recursive interpolation technique for binary images based on morphological median sets. In: Ronse Ch, Najman L, Decencire E (eds) Mathematical morphology: 40 years on. Springer, Berlin, pp 53–65